

Energy level alignment and chemical interaction at Alq₃/Co interfaces for organic spintronic devices

Y. Q. Zhan,^{1,*} M. P. de Jong,^{1,†} F. H. Li,¹ V. Dediu,² M. Fahlman,¹ and W. R. Salaneck¹

¹Department of Physics, Chemistry, and Biology, Linköping University, S-581 83 Linköping, Sweden

²Istituto per lo Studio di Materiali Nanostrutturati, Consiglio Nazionale delle Ricerche (ISMN-CNR), via Gobetti 101, 40129 Bologna, Italy

(Received 19 March 2008; revised manuscript received 10 June 2008; published 16 July 2008)

The electronic structure of the interface between tris(8-hydroxyquinoline) aluminum (Alq₃) and cobalt was investigated by means of photoelectron spectroscopy. As demonstrated recently, this interface is characterized by efficient spin injection in organic spintronic devices. A strong interface dipole that reduces the effective work function of cobalt by about 1.5 eV was observed. This leads to a large barrier for hole injection into the highest occupied molecular-orbital (HOMO) level of 2.1 eV, in agreement with a previously proposed model based on electron transport in Co-Alq₃-La_{0.7}Sr_{0.3}MnO₃ spin valves. Further experimental results indicate that chemical interaction occurs between the Alq₃ molecules and the cobalt atoms, while the latter penetrate the Alq₃ layer upon vapor deposition of Co atoms. The data presented lead to significant progress in understanding the electronic structure of the Co-on-Alq₃ interface and represent a significant step toward the definition of the interface parameters for the efficient spin injection in Alq₃ based spin valves.

DOI: 10.1103/PhysRevB.78.045208

PACS number(s): 72.80.Le, 85.75.-d, 71.20.-b, 73.40.-c

I. INTRODUCTION

Organic/ferromagnetic electrode interfaces have recently become the subject of thorough studies¹⁻⁴ because of their applications in organic spintronics.⁵⁻⁷ In this promising field, the organic semiconductors are mainly used as a spin transport layer placed between two ferromagnetic electrodes. The electronic structure of the organic/ferromagnetic electrode interface was not only found to be the main factor determining charge injection but also the possible reason for a negative spin-valve effect.⁸ Among many different organic spintronic devices, those using tris(8-hydroxyquinoline) aluminum (Alq₃, shown in Fig. 1) as a spacer between the ferromagnetic La_{0.7}Sr_{0.3}MnO₃ (LSMO) and Co electrodes have been mostly used.^{6,9,10} Recently, the alignment of energy levels at the Alq₃-on-LSMO interface was studied¹ and the existence of a strong dipole of about 0.9 eV that shifts down the energy levels of Alq₃ was reported.¹ The results indicate that electrons injected from LSMO into Alq₃ are the dominant charge carriers in the spin-valve device. However, the behavior of these spin-valve devices was only partially understood, mainly because the knowledge about the interface between cobalt electrode and the Alq₃ molecular layer was insufficient. Thus far, only the interface formed by adsorbing Alq₃-on-cobalt electrodes (Alq₃/Co) has been discussed in the literature.¹¹ In the standard organic spin-valve devices, however, cobalt is deposited onto a surface of Alq₃ (i.e., Co/Alq₃). It is well known that significantly different interfaces may be formed depending upon the order of deposition. For example, if Al atoms are deposited on LiF/Alq₃ surfaces, there is a chemical reaction between the Al atoms and the LiF (Ref. 12) that does not occur when Alq₃ atoms are deposited on Al/LiF (Ref. 13).

In this paper, the results of studies of both Co/Alq₃ and Alq₃/Co interfaces using ultraviolet and x-ray photoelectron spectroscopy (UPS and XPS, respectively) are reported. In particular, the interfacial energy level alignment at the interface of cobalt and Alq₃ is presented.

II. EXPERIMENTAL DETAILS

The experiments were carried out using a Scienta[®] ESCA 200 spectrometer. The vacuum system consists of an analysis chamber and a preparation chamber. X-ray photoelectron spectroscopy (XPS) and ultraviolet photoelectron spectroscopy (UPS) were performed in the analysis chamber at a base pressure of 10⁻¹⁰ mbar using monochromatized Al(K α) x rays at $h\nu=1486.6$ eV and He I radiation at $h\nu=21.2$ eV, respectively. The experimental conditions were such that the full width at half maximum (FWHM) of the Au 4f_{7/2} line was 0.65 eV. The binding energies were obtained referenced to the Fermi level with an error of ± 0.1 eV. Sputtering and material depositions were done in a preparation chamber with a base pressure of 10⁻¹⁰ mbar. The Alq₃ was purchased from Sigma-Aldrich. Alq₃ was deposited *in situ* from a

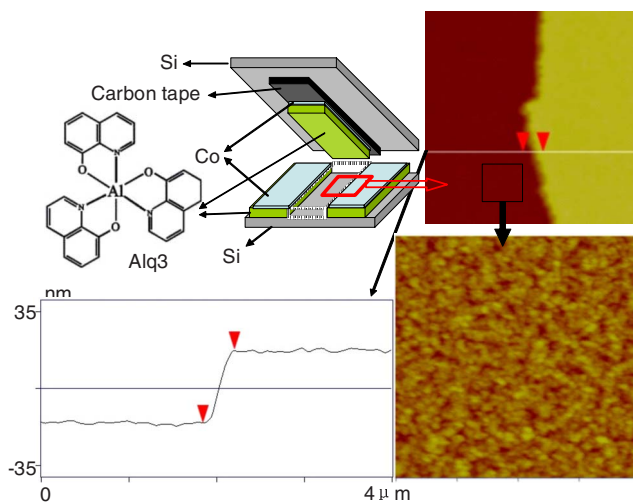


FIG. 1. (Color online) Schematic of the peel-off technique and the AFM image measured around the edge formed by the peel-off process.

simple Knudsen cell. The sublimation temperature was $\sim 280^\circ\text{C}$, resulting in a deposition rate of approximately $1 \text{ \AA}/\text{min}$ (estimated from the attenuation of the core-level signals of the bottom layer). Co atoms were deposited using an UHV e -beam evaporator (Omicron EFM3) at a deposition rate of about $3 \text{ \AA}/\text{min}$ as monitored by a quartz thickness monitor.

For the Alq_3 -on-cobalt samples (denoted as Alq_3/Co), an Au-coated Si wafer was used as the substrate, which was cleaned with an argon sputter gun until no oxygen signal was detected. As a first step, 20 nm of Co atoms were deposited on the Au-surface, where after Alq_3 films of different thickness were deposited step by step on the Co surface. Both the secondary electron cutoff (UPS) and XPS core-level spectra of Co atoms and Alq_3 were recorded for each step. For investigating the cobalt-on- Alq_3 (denoted as Co/Alq_3) interface, first a 15-nm-thick Alq_3 film was deposited on a sputter-cleaned Si substrate followed by deposition of 20 nm Co atoms. Afterward, the sample was removed from vacuum and a simple *ex situ* peel-off technique was adopted to turn over the Co/Alq_3 sample—a technique described in the literature.¹⁴ A clean Si substrate attached to a two-sided UHV-compatible conductive carbon tape was pressed onto the $\text{Co}/\text{Alq}_3/\text{Si}$ sample in the atmosphere. After separating the two Si substrates, the Co/Alq_3 sample was peeled off from the Si substrate and attached to the carbon tape (as illustrated in Fig. 1). Because of the poor adhesion between Alq_3 molecules and the Si substrate,¹⁵ the peel-off process is quite reproducible. XPS measurements confirmed that there were no significant amounts of Alq_3 or cobalt left on the substrate, which indicates that separation occurred at the Alq_3/Si interface. The advantage of the peel-off procedure with respect to the various *in situ* etching techniques is that it maintains the interface morphology intact. The bare Si surface, after the Co/Alq_3 multilayer has been peeled off, was also studied by atomic force microscopy (AFM). The inverted sample, now Co/Alq_3 tape, was transferred back into vacuum and analyzed by XPS and UPS. Angle-resolved XPS spectra of the inverted sample were measured as well. The take-off angle, noted in the figure, is defined (by Scienta AB) as the angle between the direction of the detected electrons and the surface of the sample, i.e., a 90° take-off angle means that the electrons are detected leaving perpendicular to the surface (parallel to the surface normal). For a given electron energy, varying the take-off angle changes the effective escape depth (inelastic elastic mean-free path λ) between its full value at $\varphi=90^\circ$ and a minimum at glancing take-off angles. The λ values used in the analysis are calculated by TPP-2M equation.¹⁶

III. RESULTS AND DISCUSSION

In Fig. 1, the *ex situ* peel-off process is illustrated at the top left corner. For the case where part of the Co/Alq_3 layer was peeled off, the residual substrate was studied by AFM. An AFM image of $4 \times 4 \mu\text{m}^2$ area around the edge formed by the peel-off process is shown at the top right corner of the figure. The dark part of the image represents the area on which the Co/Alq_3 layer has been peeled off, while the

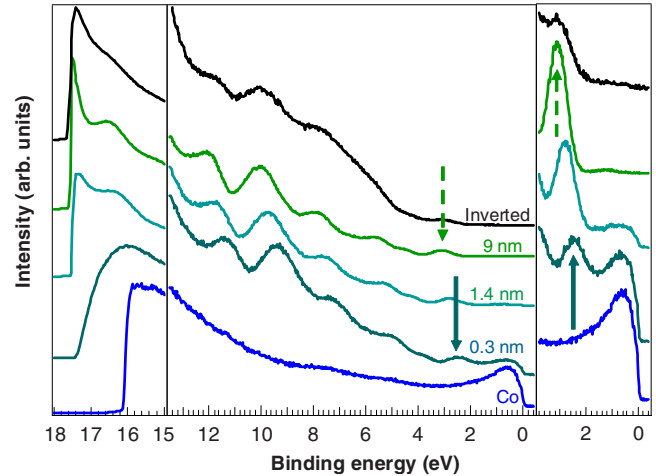


FIG. 2. (Color online) Secondary electron cutoffs at both Alq_3/Co and inverted (i.e., Co/Alq_3) interfaces. Inset: Valence-band photoelectron spectra at both Alq_3/Co and Co/Alq_3 interfaces. The energy positions of the HOMO are indicated by arrows as discussed in the text.

bright part represents the area that is still covered by the Co/Alq_3 layer. It clearly shows that a sharp boundary was formed by the peel-off process. The height profile across the boundary is shown at the bottom left corner of Fig. 1. The height difference between the two arrows is $33 \pm 3 \text{ nm}$, which is in good agreement with the thickness of the Co/Alq_3 layer before the peel-off process ($35 \text{ nm} \pm 3$). This confirms that the separation of the peel off occurs abruptly at the Alq_3/Si interface. Another AFM image of a $1 \times 1 \mu\text{m}^2$ remnant area after peel off is shown at the bottom right corner of Fig. 1. The root mean-square (rms) roughness is $0.60 \pm 0.06 \text{ nm}$, which is fairly smooth. Furthermore, no isolated islands could be found on the remnant area, which indicates that the Alq_3 layer on the inverted sample is still quite homogeneous and that the cobalt should still be fully covered by the Alq_3 layer.

The UPS spectra of both Co/Alq_3 and inverted (Alq_3/Co) interfaces are shown in Fig. 2. The spectrum denoted by “Co” corresponds to the clean 20-nm-thick Co film, while spectra denoted by a certain thickness (e.g., 0.3 nm) refer to the cobalt film covered by an Alq_3 layer of that thickness ($0.3 \pm 0.03 \text{ nm}$), and the spectrum denoted by “Inverted” refers to the inverted, i.e., Co/Alq_3 interface. The spectra both in the left (the secondary electron cutoffs) and right (Fermi levels and HOMOs) panels follow the same order as in the center panel. First, looking at the left panel of Fig. 2, by subtracting the binding energy of the cutoff from the excitation energy, the work function of the as-deposited Co film was about $5.0 (\pm 0.1) \text{ eV}$, which is in good agreement with previously published values.^{11,17} A sudden change of 1.3 eV in the secondary electron cutoff occurs upon deposition of the very first (submono) layer of Alq_3 , where the average thickness is estimated to be 0.3 nm. By depositing an additional 1.2 nm of Alq_3 on the surface, the secondary electron cutoff shifts slightly by an additional 0.2 eV toward higher binding energy. From a thickness of about 0.3–9 nm, the work function remains constant at about 3.6 eV. In the case

of an inverted sample (i.e., Co/Alq₃), the slope of the secondary electron cutoff is slightly different from that of an Alq₃/Co sample, most probably related to surface roughness. However, the work function is the same (about 3.6 eV).

For both cases, Co/Alq₃ and Alq₃/Co, even though the sharpness of the interface may not be the same, there is a 1.5 eV decrease in the work function of Co, which corresponds to the formation of an interfacial dipole with the positive charge at the Alq₃ side. This strong interface dipole rigidly shifts the valence features of Alq₃ toward higher binding energy. It is unlikely that this dipole results from integer electron donation from Alq₃ to Co (Refs. 18 and 19) since the first ionization potential of Alq₃ is so large (about 5.7 eV). Instead, the dipole most probably originates from the strong intrinsic dipole moment of the Alq₃ molecule. As discussed in a previous paper,¹ a fully ordered Alq₃ layer could result in a shift of about 1 eV, arising from the intrinsic dipoles of Alq₃ molecules. In the present case, an additional lowering of the work function resulting from Pauli repulsion is expected²⁰ on the order of several tenths of an eV. The 1.5 eV shift is thus rational in terms of Pauli repulsion in combination with (partial) ordering of the Alq₃ dipoles at the interface. Given the fact that the observed shift is similar for both Alq₃/Co and Co/Alq₃ interfaces, such an ordering of molecular dipoles must come about via a rather strong interaction between Co atoms and Alq₃ molecules, since no pre-existing dipole ordering exists at the Alq₃ surface prior to deposition of Co atoms. For Alq₃-on-Al surfaces, theoretical studies have shown that the Alq₃ molecules interact with the substrate via their oxygen atoms.²¹ The stable adsorbate geometries feature strong dipole moments that act to decrease the work function of the Al substrate, as also found in experiments.²² A similar scenario may apply to Alq₃ on Co and Co on Alq₃.

In Fig. 2, center panel, it may be seen that as Alq₃ is slowly deposited on the surface of the Co substrate (Alq₃/Co), the electronic structure of the Alq₃ molecules appeared already for the average thickness of 0.3 nm, superimposed on the Co spectrum. The initial position of the HOMO peak is indicated by the solid arrow. With increasing the thickness of Alq₃, up to 9 nm average thickness, the energy of the HOMO-peak shifts toward high binding energy (dashed arrow in the figure), and the signal from the Fermi edge of the substrate disappears. For the inverted sample (Co/Alq₃), all of the Alq₃ features are still visible and at the same position as for the Alq₃/Co sample with 9 nm Alq₃, showing no change of the electronic structure after the peel-off process. There is no intensity at the Fermi edge in the valence-band spectra of both the Alq₃/Co and the inverted Co/Alq₃ interfaces, indicating that the Co film is fully covered by Alq₃ in both samples. In the case of the inverted interface (Co/Alq₃), the full coverage by Alq₃ confirms that the peel-off process has not detached Co molecules from the Alq₃ film and that the separation occurs at the Alq₃/Si interface.

From the data obtained from inverted (Co/Alq₃) interfaces, the energy level alignment at the interface of Co on Alq₃ may be constructed. In combination with previous results on the Alq₃/LSMO interface,¹ the energy level diagram of a complete typical organic spin-valve device

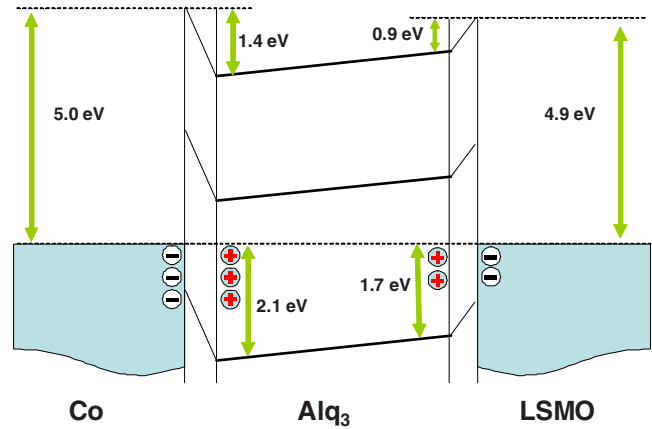


FIG. 3. (Color online) Schematic of energy band of the standard LSMO/Alq₃/Co spin-valve devices.

(Co/Alq₃/LSMO) is shown in Fig. 3. The work function of Co is 5.0 ± 0.1 eV, which is slightly higher than that of LSMO (4.9 eV) (Ref. 1) since the HOMO level of Alq₃ is 2.1 ± 0.1 eV higher in binding energy (leading edge of the HOMO peak) relative to the Fermi level—that is 3.6 ± 0.1 eV below the vacuum level. Thus the ionization potential is 5.7 ± 0.2 eV, which is in good agreement with our previous results¹ and other reported values.^{1,23} The vacuum level offset at the interface between Alq₃ and Co is 1.4 ± 0.1 eV, obtained by subtracting the work function of the inverted sample (Co/Alq₃) from that of Co. The 1.4 eV vacuum level difference of the Co/Alq₃ interface is 0.5 eV larger than that of the LSMO/Alq₃ interface.¹ By subtracting the vacuum level difference of the two electrodes, a 0.4 ± 0.2 eV built-in potential difference, inside the spin-valve device, is obtained (see Fig. 3). An asymmetric IV characteristic of the device in this structure is consequently expected. However, a nearly symmetric IV curve has been reported by Xiong *et al.*⁶ and furthermore, the main spin-valve effect takes place for applied voltages below 0.2 V. This result is in contrast with nearly symmetric IV curves that have been mainly observed and with the fact that the spin-valve effect is detected at low applied voltages of about 1 V (Refs. 6, 8, and 9). This discrepancy indicates that our knowledge on spin injection at organic-inorganic interface is still very poor and that additional mechanisms for the spin polarized electron injection and transport at the range of very low operating voltage must be also considered.

Looking closer at the energy level alignment of the two electrode interfaces, if either the optical gap (2.8 eV) (Ref. 23) or the HOMO-LUMO (lowest unoccupied molecular-orbital) splitting measured directly by scanning tunneling spectra (STS) (2.96 ± 0.13 eV) (Refs. 24 and 25) is used to estimate the HOMO-LUMO gap, the injection barrier for electrons is much smaller than that for holes. The same configuration (electron injection favored) was found for the Alq₃/LSMO interface.¹ Therefore, the dominant charge carriers in the Co/Alq₃/LSMO (i.e., Co-on-Alq₃-LSMO) spin-valve devices should be electrons. A recent paper claims the hole injection is easier than electron injection at Alq₃/Co interface²⁶ based on the IV characteristic of their device, which is contrary to the well-known electron-transport nature

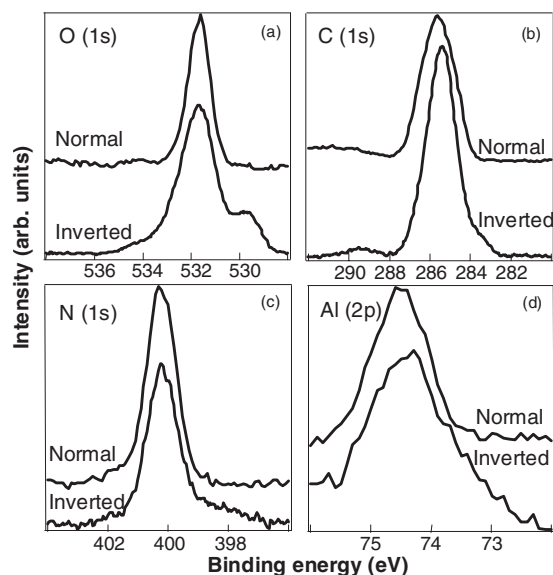


FIG. 4. Photoelectron spectra of O(1s), C(1s), N(1s), and Al(2p) levels at the Alq₃/Co interface compared to the corresponding spectra of solid Alq₃.

of Alq₃ and other published results. Moreover, the light emission from Co/Alq₃/indium tin oxide (ITO) device, reported by Xiong *et al.*,⁶ confirms in a straightforward way that the electron injection at Co/Alq₃ interface is possible. Efficient light emission has also been detected by injecting electrons through Co/LiF/Al interface.²⁷

In addition to the above described energy level alignment, possible chemical interactions at the interface have also been studied by recording the XPS core-level spectra of both Alq₃ and Co. Figure 4 shows the O(1s), C(1s), N(1s), and Al(2p) spectra of the inverted sample interface (labeled as “Inverted”) compared to the corresponding spectra for an Alq₃ film (labeled as “Normal”). In the O(1s) spectrum of the pure Alq₃ film, there is only one peak located at 531.6 eV. However, two peaks are observed in the O(1s) spectrum of the inverted sample. Using a Gaussian multiplex fitting, the positions of the two peaks could be estimated. The main peak is at almost the same position (531.9 eV) as that for solid Alq₃, while the position of the additional peak is 529.6 eV, located at the low binding-energy side of the main peak. The appearance of the additional O(1s) peak correlates with extra features in the Co core-level spectra (Fig. 5), showing that significant chemical interaction takes place between Co and O atoms in the Alq₃ film on an inverted sample (i.e., Co/Alq₃). There are two possibilities. First, the oxidation of Co atoms might occur when Co atoms are deposited onto Alq₃. Cobalt atoms at or near the interface might interact with the oxygen atoms of Alq₃ molecules. Second, the oxidation might occur during the *ex situ* peel-off process. The oxygen in the air could diffuse into the organic layer, reach the Co-Alq₃ interface, and oxidize the cobalt atoms near the. The former case represents a chemical reaction between Co atoms and Alq₃ molecules. This latter (second) possibility appears to be the case, since a new shoulder formed on the low binding-energy side of the C(1s) peak of the inverted sample interface (top right panel). The main C(1s) peak

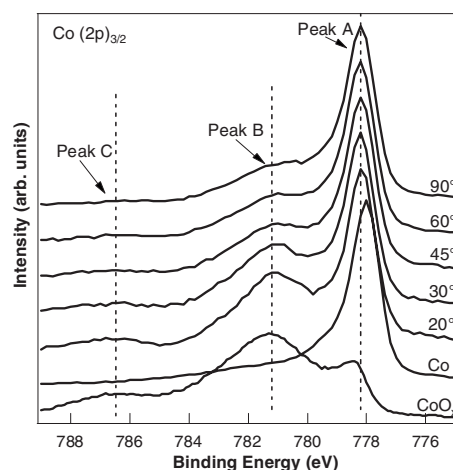


FIG. 5. Angle-resolved photoelectron spectra of Co(2p_{3/2}) at the inverted (i.e., Co/Alq₃) interfaces.

(285.4 eV) is at the same binding energy as the single C(1s) peak (285.6 eV) of the pure Alq₃.

To provide additional confirmation of the interaction between Co atoms and Alq₃ molecules, a submonolayer of cobalt (equivalent to a deposition thickness of 0.2 nm) deposited on Alq₃ was studied. The Co(2p)_{3/2} spectrum of such an “ultrathin” Co layer on Alq₃, shown in Fig. 6, is in comparison with the Co(2p)_{3/2} spectrum of a pure cobalt layer (labeled as “Normal”). In addition to the main Co(2p)_{3/2} peak, a shoulder at about 782 eV is clearly visible. The position of the shoulder is consistent with that of peak B in Fig. 5. This supports the conclusion that the additional peaks in the O(1s) and Co(2p) spectra of the inverted sample are indicative of Co-Alq₃ interactions, even though additional oxidation during the *ex situ* peel-off process cannot be ruled out completely. Returning to the N(1s) and Al(2p) spectra also shown in Fig. 4, there are no significant differences between the spectra for the inverted sample interface and those for a pure Alq₃ film, suggesting that Co atoms do not interact directly with the pyridyl ligands of the Alq₃ molecules.

In Fig. 5, the angle-dependent XPS Co(2p)_{3/2} spectra of an inverted sample are shown and labeled by the take-off

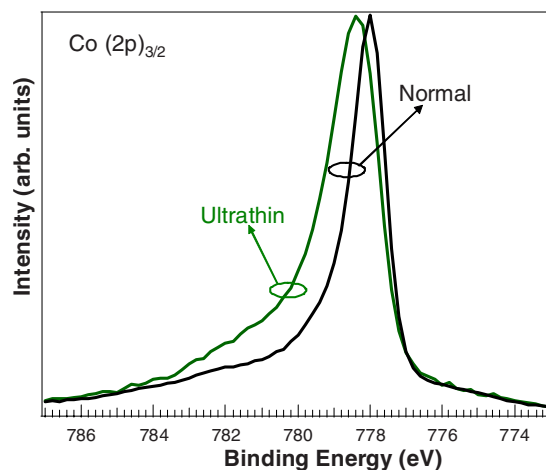


FIG. 6. (Color online) Photoelectron spectra of Co(2p)_{3/2} of an ultrathin cobalt submonolayer (0.2 nm) deposited onto Alq₃.

angles. As references, $\text{Co}(2p)_{3/2}$ spectra of both pure cobalt and native cobalt oxide²⁸ are also shown and labeled as “Co” and “ CoO_x .” By comparing the 90° $\text{Co}(2p)_{3/2}$ spectra of the inverted sample with the $\text{Co}(2p)_{3/2}$ spectra of pure cobalt, at least one new peak (peak *B*) appears near 781.2 eV. The main peak (*A*) at 778.2 eV is approximately equal in binding energy to the binding energy of the single peak for pure (metallic) Co (778 eV). Upon decreasing the take-off angle, the relative intensity of peak *B* compared to peak *A* increases, and a new peak (peak *C*) appears near 786.5 eV. At a take-off angle of 20° , i.e., the most surface sensitive mode, the $\text{Co}(2p)_{3/2}$ spectra of inverted sample is a clear three-peak structure, and the peaks *B* and *C* match very well with the corresponding peaks in the spectrum of native cobalt oxide. Therefore, the main peak *A* is identified as the single peak of pure metallic cobalt with a small contribution from a native cobalt oxide.

In an inverted sample, the cobalt layer is fully covered by about 15 nm of AlQ_3 , as indicated by both AFM measurement and UPS data. The $\text{Co}(2p)$ peak therefore is extremely weak. Since $\lambda \approx 2.1$ nm (calculated by TPP-2M equation¹⁶) for electrons emitted from the $\text{Co}(2p)$ level, for an over-layer thickness of AlQ_3 atoms equivalent to about 7λ , the $\text{Co}(2p)$ peak intensity should be reduced to about 0.1% of the intensity of an uncovered Co surface). However, the $\text{Co}(2p)$ peak for an inverted sample is fairly strong (20% of the intensity of the bare Co surface). Thus, it appears that the cobalt atoms penetrate into the AlQ_3 layer during the deposition. The increase in the relative intensities of peaks *B* and *C* compared to peak *A* for surface sensitive spectra is a consequence of this penetration or diffusion of Co atoms (more likely, clusters) during the vapor deposition. The degree of penetration of cobalt atoms is obviously related to the size of cobalt clusters. The relative intensity of $\text{Co}(2p)$ peaks corresponding to a cobalt oxide increases upon increased surface sensitivity as in the intensity of peaks *B* and *C* in the figure. This indicates a penetration of Co atoms or clusters into the AlQ_3 film followed by phenoxide interaction. A possible method for limiting the penetration of Co atoms has been reported recently by Riminucci *et al.*⁸ In their device, a thin Al_2O_3 layer has been inserted between AlQ_3 and Co.

IV. SUMMARY

The electronic structure of the AlQ_3 -Co interface was investigated by means of photoelectron spectroscopy. An interfacial dipole of about 1.5 eV was observed in a direction that results in a shift of the whole energy-band edges of the AlQ_3 over layer to higher binding energies with respect to the vacuum level. This results in a barrier for the hole injection of about 2.1 eV, leading to the dominance of electron transport in spintronic devices incorporating these interfaces. Looking at the complete LSMO/ AlQ_3 /Co device, the UPS results indicate a built-in potential of 0.4 ± 0.2 eV. The previously reported spin-valve effect occurred for applied potentials smaller than 0.2 eV (Ref. 6), however, suggested an additional mechanisms for the spin polarized electron injection and transport at the range of very low operating voltage. Furthermore, core-level XPS spectra of both AlQ_3 and cobalt indicate that cobalt atoms (clusters) penetrate into the AlQ_3 layer upon the vapor deposition and chemical react with the phenoxide part of the AlQ_3 molecules at and near the interface. The present results not only contribute to a quantitative description of organic spintronic devices that incorporate AlQ_3 -Co interfaces, but also illustrate the importance of studying the other actual organic-ferromagnetic metal interface in organic spintronic device,²⁹ as constructing energy diagrams based on work functions and HOMO/LUMO positions of the individual components will not give the correct energy level alignment.^{16,17}

ACKNOWLEDGMENTS

The authors acknowledge financial support from the EU (FW6, STREP) OFSPIN project. The LiU authors acknowledge the financial support from the Swedish Research Council (VR) with indirectly funded project grants as well as a Linneus Center grant, the Knut and Alice Wallenberg Foundation, the Carl Tryggers Foundation, and the Center for Advanced Molecular Materials, CAMM, funded by the Swedish Foundation for Strategic Research, SSF.

*yiqzh@ifm.liu.se

†Present address: MESA+ Institute for Nanotechnology, University of Twente 7500 AE Enschede, The Netherlands

¹Y. Q. Zhan, I. Bergenti, L. E. Hueso, and V. Dediu, *Phys. Rev. B* **76**, 045406 (2007).

²J. H. Seo, S. J. Kang, C. Y. Kim, K. H. Yoo, and C. N. Whang, *J. Phys.: Condens. Matter* **18**, S2055 (2006).

³M. Popinciuc, H. T. Jonkman, and B. J. van Wees, *J. Appl. Phys.* **100**, 093714 (2006).

⁴M. Popinciuc, H. T. Jonkman, and B. J. van Wees, *J. Appl. Phys.* **101**, 093701 (2007).

⁵V. Dediu, M. Murgia, F. C. Maticotta, C. Taliani, and S. Barbanera, *Solid State Commun.* **122**, 181 (2002).

⁶Z. H. Xiong, D. Wu, Z. V. Vardeny, and J. Shi, *Nature (London)*

427, 821 (2004).

⁷T. S. Santos, J. S. Lee, P. Migdal, I. C. Lekshmi, B. Satpati, and J. S. Moodera, *Phys. Rev. Lett.* **98**, 016601 (2007).

⁸A. Riminucci, I. Bergenti, L. E. Hueso, M. Murgia, C. Taliani, Y. Zhan, F. Casoli, M. P. de Jong, and V. Dediu, arXiv:cond-mat/0701603 (unpublished).

⁹W. Xu, G. J. Szulczewski, P. Leclair, I. Navarrete, R. Schad, G. Miao, H. Guo, and A. Gupta, *Appl. Phys. Lett.* **90**, 072506 (2007).

¹⁰S. Majumdar, H. S. Majumdar, R. Laiho, and R. Österbacka, *J. Alloys Compd.* **423**, 169 (2006).

¹¹A. N. Caruso, D. L. Schulz, and P. A. Dowben, *Chem. Phys. Lett.* **413**, 321 (2005).

¹²C. I. Wu, G. R. Lee, and T. W. Pi, *Appl. Phys. Lett.* **87**, 212108

- (2005).
- ¹³S. K. M. Jonsson, W. R. Salaneck, and M. Fahman, *J. Appl. Phys.* **98**, 14901 (2005).
- ¹⁴H. J. Shin, M. C. Jung, J. Chung, K. Kim, J. C. Lee, and S. P. Lee, *Appl. Phys. Lett.* **89**, 063503 (2006).
- ¹⁵J. K. Kim, J. W. Park, and K. Y. Suh, *Key Eng. Mater.* **339**, 469 (2007).
- ¹⁶S. Tanuma, C. J. Powell, and D. R. Penn, *Surf. Interface Anal.* **21**, 165 (1994).
- ¹⁷H. B. Michaelson, *J. Appl. Phys.* **48**, 4729 (1977).
- ¹⁸C. Tengstedt, W. Osikowicz, W. R. Salaneck, I. D. Parker, C.-H. Hsu, and M. Fahlman, *Appl. Phys. Lett.* **88**, 053502 (2006).
- ¹⁹M. Fahlman, A. Crispin, X. Crispin, S. K. M. Henze, M. P. de Jong, W. Osikowicz, C. Tengstedt, and W. R. Salaneck, *J. Phys.: Condens. Matter* **19**, 183202 (2007).
- ²⁰V. De Renzi, R. Rousseau, D. Marchetto, R. Biagi, S. Scandolo, and U. del Pennino, *Phys. Rev. Lett.* **95**, 046804 (2005).
- ²¹S. Yanagisawa and Y. Morikawa, *Chem. Phys. Lett.* **420**, 523 (2006).
- ²²H. Ishii, K. Sugiyama, E. Ito, and K. Seki, *Adv. Mater. (Weinheim, Ger.)* **11**, 605 (1999).
- ²³S. T. Lee, X. Y. Hou, M. G. Mason, and C. W. Tang, *Appl. Phys. Lett.* **72**, 1593 (1998).
- ²⁴S. F. Alvarado, L. Libioulle, and P. F. Seidler, *Synth. Met.* **91**, 69 (1997).
- ²⁵S. F. Alvarado, L. Rossi, P. Muller, P. F. Seidler, and W. Riess, *IBM J. Res. Dev.* **45**, 89 (2001).
- ²⁶J. S. Jiang, J. E. Pearson, and S. D. Bader, *Phys. Rev. B* **77**, 035303 (2008).
- ²⁷I. Bergenti, V. Dediu, E. Arisi, T. Mertelj, M. Murgia, A. Riminucci, G. Ruani, M. Solzi, and C. Taliani, *Org. Electron.* **5**, 309 (2004).
- ²⁸B. V. Crist, *Handbook of Monochromatic XPS Spectra, The Elements of Native Oxides* (Wiley, Chichester, 2000).
- ²⁹F. J. Wang, C. G. Yang, Z. V. Vardeny, and X. G. Li, *Phys. Rev. B* **75**, 245324 (2007).